Radiocarbon (2026), **68**, pp. 382–391
doi:10.1017/RDC.2026.10195

CAMBRIDGE UNIVERSITY PRESS

RESEARCH ARTICLE

Early ^{14}C increase in high-latitude trees at 665–664 BC

Junghun Park[1], Joonas Uusitalo[2], Wan Hong[1], Gyujun Park[1], Kilho Sung[3], Thomas Hackman[4], Samuli Helama[5], Harri Mäkinen[6], Pekka Nöjd[6] and Markku Oinonen[2]

[1]Korea Institute of Geoscience and Mineral Resources, Geoanalysis Center, Republic of Korea, [2]Finnish Museum of Natural History, University of Helsinki, Helsinki, Finland, [3]GNS, Gracefield, Lower Hutt, New Zealand, [4]Department of Physics, University of Helsinki, Helsinki, Finland, [5]Natural Resources Institute Finland, Rovaniemi, Finland and [6]Natural Resources Institute Finland, Helsinki, Finland

Corresponding author: Joonas Uusitalo; Email: joonas.uusitalo@helsinki.fi

Received: 01 October 2025; **Revised:** 10 December 2025; **Accepted:** 12 December 2025; **First published online:** 03 March 2026

Keywords: 660 BC; Arctic; dendrochronology; intra-annual radiocarbon measurement; Solar Proton Event; Δ^{14}C peak

Abstract

The discovery of radiocarbon (^{14}C) peaks in AD 774–775 and AD 993–994 sparked the search for other anomalous events, leading to the identification of one around 660 BC. However, the ~660 BC event appears to show a more prolonged increase, raising the question whether the event is qualitatively different. To investigate this, we measured high-latitude tree rings from Finnish Lapland, expected to be highly sensitive to energetic particle events. We measured the ^{14}C content of full rings, as well as their separated earlywood and latewood components. We found that the ^{14}C concentrations start rising already in the latewood of 665 BC and reach almost its full intensity by 664 BC. This rapid increase is similar to that at another high-latitude site (Yamal, Russia) but contrasts with that of low-latitude sites, which show a later peak. The earlier increase of the ^{14}C at high-latitude tree rings compared to lower latitudes is consistent with similar observations for the AD 774 and AD 993 Miyake events. Based on carbon-cycle box modeling, the structure of the subsequent amplitude increase can be explained by either single or double initial ^{14}C pulses. The fast increase coupled with a slower subsequent peak structure suggests similar mechanisms behind the high-latitude observations, i.e., tropospheric ^{14}C production and/or a fast component of polar air flow across the tropopause combined with the full stratospheric-tropospheric CO_2 exchange. Our results strongly emphasize the need for dynamic carbon cycle models to understand the observed differences between high- and lower-latitude data.

Introduction

Following the discovery of a rapid rise of radiocarbon (^{14}C) concentrations in tree rings of AD774/5 (M12) (Büntgen et al. 2018; Güttler et al. 2015; Miyake et al. 2012; Park et al. 2017; Uusitalo et al. 2018), other similar Δ^{14}C peaks have been studied, including AD 993/4 (Miyake et al. 2013), 5480 BC (Miyake et al. 2017), ~660 BC (O'Hare et al. 2019; Park et al. 2017; Sakurai et al. 2020), 813 BC (Jull et al. 2018), AD 1052/1054 (Brehm et al. 2021; Terrasi et al. 2020), 5410 BC (Miyake et al. 2021), AD 1279 (Brehm et al. 2021; Miyahara et al. 2022), 7176 BC (Brehm et al. 2022; Paleari et al. 2022), 5259 BC (Brehm et al. 2022), and 12351 BC (Bard et al. 2023). Since the initial discovery, several hypotheses have been proposed to explain their cause, including solar proton events (SPEs) (Jull et al. 2014; Mekhaldi et al. 2015; Melott and Thomas 2012; Miyake et al. 2012; Usoskin et al. 2013), supernova (Miyake et al. 2012), and gamma-ray explosions (Hambaryan and Neuhäuser 2013; Pavlov et al. 2013). However, with subsequent discoveries, the scientific consensus has shifted towards SPEs as the most likely explanation, a conclusion strongly supported by corresponding bipolar ^{10}Be measurements from ice cores (Mekhaldi et al. 2015). While SPE hypothesis accounts for most of the events, the ones dated to 5480 BC and 813 BC appear to have a longer duration. This has led to suggestions that these longer-

© The Author(s), 2026. Published by Cambridge University Press on behalf of University of Arizona. This is an Open Access article, distributed under the terms of the Creative Commons Attribution licence (https://creativecommons.org/licenses/by/4.0/), which permits unrestricted re-use, distribution and reproduction, provided the original article is properly cited.

Check for updates

lasting phenomena might be connected to special modes of grand solar minimum (Jull et al. 2018; Miyake et al. 2017).

In this work, our focus is on the ~660 BC peak and its comparison to other overlapping data sets and of AD774, in particular. The event is particularly intriguing as it also has an apparently longer rise time compared to most of the other events (Park et al. 2017). To explain this prolonged duration, a double SPE or an extended production period has been proposed (Park et al. 2017; Sakurai et al. 2020). More exotically, Pavlov et al. (2019) have suggested that the prolonged rise could have resulted from a solar system encounter with an interstellar gas cloud and the resulting compression of the heliosphere and enhanced galactic cosmic ray flux. To examine the ~660 BC event in more detail, we use high-latitude tree rings from Finland, which previously have been found to be sensitive to such an event (Miyake et al. 2022; Uusitalo et al. 2018). Variations in the shape of the $\Delta^{14}C$ peak across geographical regions could provide valuable insights into the structure and type of the ~660 BC event.

Samples and methods

Tree-ring samples of Scots pine (*Pinus sylvestris*) were collected in Lapland (Hangasjärvi, Salla; 66.8° N, 28.7°E), Finland. In this region, the periods of earlywood (early June to early July; EW) and latewood growth (late June to late August, LW) are very short, thus recording tropospheric ^{14}C contents within a very narrow time window. The collection, cross-dating, slicing, and cellulose extraction of the samples into α-cellulose are detailed in Uusitalo et al. (2022). This process was conducted by the Finnish Tree-Ring Research Consortium (FITRE) at the University of Helsinki and the Natural Resources Institute Finland. The α-cellulose samples were combusted, converted chemically to graphite targets, and measured for ^{14}C using the accelerator mass spectrometry facility at the Korean Institute of Geoscience and Mineral Resources in Daejeon, Korea (Hong et al. 2010a, 2010b). The results are reported as decay-corrected $\Delta^{14}C$ values, hereafter as $\Delta^{14}C$. To take into account potential baseline offsets in illustrations, the data was also normalized by shifting the mean $\Delta^{14}C$ value of 4 years predating the anomaly (669–666 BC and AD 770–773) to $\Delta^{14}C = 0$ (see Tables S1 and S2).

The tree-ring data were supported by an 11-box global carbon cycle box model (Güttler et al. 2015) studies to estimate the amplitude and timing of the required ^{14}C production. This simulation used a daily time resolution, in contrast to the monthly resolution used by other researchers, as the typical duration of a SPE is only a few days. In order to maintain a stable ^{14}C amount in the troposphere, the annual production amount of ^{14}C in the atmosphere is calculated to be 6.8kg, and this amount is used consistently during the simulation. However, this amount is modulated by the sinusoidal signal of the solar cycle with a period 11 years (Güttler et al. 2015), and is described as $P_{mod} = P_M + P_{S,C} \cdot P_M \cdot \sin(2\pi/T \cdot y + \varphi)$, where T denotes the cycle-length (11 yr)., y is the year, P_M is the average annual production amount of ^{14}C in the atmosphere (6.8kg), $P_{S,C}$ is solar cycle amplitude adopted as 18% and φ is the phase. During the simulation, the solar cycle amplitude ($P_{S,C}$) and phase (φ) are scanned. This simulation uses an oxidation time of 3.8 months for ^{14}C, indicating the time required for the oxidation of ^{14}C produced by SPE (Park et al. 2020). This oxidation time can cause a corresponding delay from the SPE occurrence to the time at which $\Delta^{14}C$ signal appears in the tree rings. Previous studies have employed a 30% tropospheric production ratio for ^{14}C (Güttler et al. 2015; Sakurai et al. 2020). This value is appropriate for production driven by Galactic Cosmic Rays (GCRs), as their high energy facilitates deep penetration into the atmosphere. However, for solar cosmic rays (SCRs), it is likely an overestimation. Recent simulations indicate a more realistic range for SCR-induced production is between 0.54% and 12% (Golubenko et al. 2022; Hyo Min and Junghun 2022). Therefore, we adopt the upper bound of 12%. This value allows for significant tropospheric production, in line with previous analyses, while remaining within the realistic range based on the current best understanding of SCR-induced production.

https://doi.org/10.1017/RDC.2026.10195 Published online by Cambridge University Press

Figure 1. *Tree-ring samples of Scots pine (Pinus sylvestris) were collected in Lapland (Hangasjärvi, Salla; 66.8°N, 28.7E, red dot), Finland.*

Result and discussion

$\Delta^{14}C$ values of annual (680–650 BC) and subannual (670–655 BC) tree-ring samples from Finland are given in Supplementary Information Tables S1 and S2 and depicted in Figure 2. There is a baseline difference between the $\Delta^{14}C$ of annual and subannual tree-ring data, which has been normalized to zero using pre-event values (see Figure 2 captions). The subannual data show a slight increase of ∼5‰ already in latewood of 665 BC. The $\Delta^{14}C$ values increase in both annual and subannual data in 664 BC and reach their maximum in 662–661 BC. The maximum is followed by a slow decline with occasional deviations, particularly in 655 BC when absolute annual and subannual values differ by ∼5‰, which in Figure 2 get amplified to nearly 10‰ due to normalization (see Table S2).

Altogether, 11 out of 16 subannual measurement pairs show larger $\Delta^{14}C_{LW}$ compared to $\Delta^{14}C_{EW}$ by 0.3–5.1‰ (see Table S2). Such variation could be attributed to a multitude of factors. ^{14}C concentrations in the troposphere are slightly higher during the period when latewood forms (August–September) than during earlywood (April–July), as the exchange between the stratosphere and troposphere is more pronounced during the spring/summer of the Northern Hemisphere (Nydal et al. 1968; Yasuike et al. 2008). For instance, seasonal variation causes 10-20% fluctuation of the tropospheric bomb peak (Hua et al. 2013; Levin et al. 1985) observed after the peak maximum. Fluctuation of similar magnitude

https://doi.org/10.1017/RDC.2026.10195 Published online by Cambridge University Press

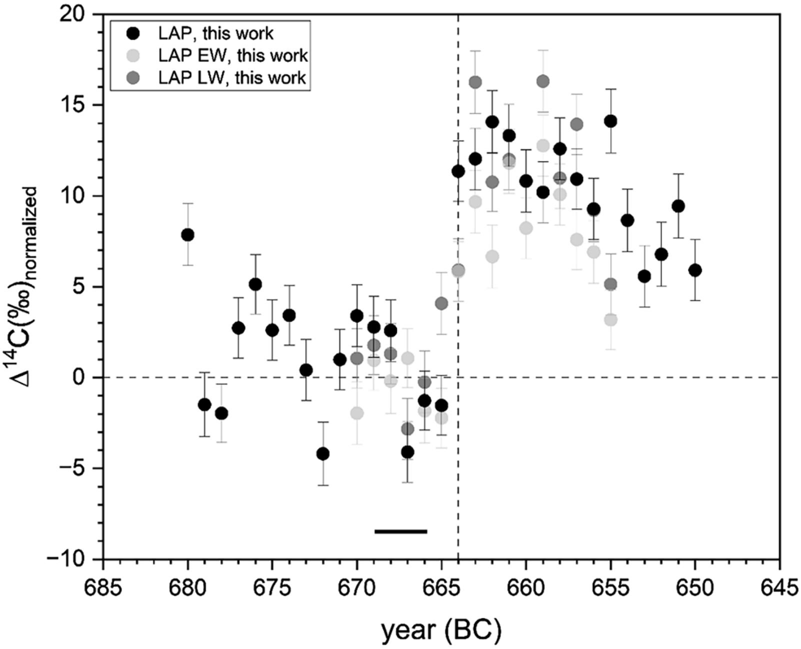

Figure 2. *$\Delta^{14}C_{normalized}$ of annual and subannual data from tree rings of Finnish Lapland (LAP) plotted against years (BC). The data has been normalized by setting the mean of 669–666 BC to equal to 0 to remove potential baseline differences. The dashed horizontal and vertical lines are for guiding the eye corresponding to the zero baseline and the year 664 BC, respectively. The horizontal solid line shows the years used for normalization.*

would mean a 1.5–3‰ annual tropospheric ^{14}C variation due to the ~15‰ 660 BC event after the peak maximum. Thus, we suggest this trend of $\Delta^{14}C_{LW} > \Delta^{14}C_{EW}$ is partly due to seasonal variation coupled to the peak intensity changes. Indeed, before the assumed SPE in 670–666 BC the LW-EW differences seem to be smaller, ranging from 0.3 to 1.7‰. Therefore, we propose that the ~5‰ rise of $\Delta^{14}C_{LW}$ in 665 BC may not only be due to seasonal variation but it could include pure SPE-induced ^{14}C increase, as well. This rise appears to form the leading edge of the increasing ^{14}C signal that subsequently continues for several years.

When normalized, high-latitude Δ^{14}C data from Lapland (LAP) and Yamal (YAM; Panyushkina et al. 2024) appear elevated compared to lower-latitude data from Altai (ALT; Panyushkina et al. 2024), Germany (GER; Park et al. 2017), and Japan (JAP; Sakurai et al. 2020), as shown in Figure 3. Furthermore, the ^{14}C rise in the Lapland and Yamal data begins earlier than in the lower-latitude data: in 664 BC, values at LAP and YAM are 11–13‰ above the baseline, whereas values at the lower-latitude sites are only 0–7‰. We also note a difference in the baselines; without normalization, the Δ^{14}C values before the event, particularly for ALT and GER, are clearly above 0‰, while lower values are observed at LAP and YAM. This feature is interesting in itself and leads to larger peak amplitude differences after normalization. Therefore, these data suggest that the high-latitude Δ^{14}C rise seems to be faster and that the amplitude and full magnitude of the signal seem to be larger than at lower latitudes.

There are two possible explanations for the fast rise of the signal at high latitudes that may contribute in parallel. First, ^{14}C produced in the high-latitude troposphere may directly affect Δ^{14}C in the high-latitude tree rings. ^{14}C is primarily produced in polar areas, with up to 12% possibly generated in the polar troposphere (Golubenko et al. 2022; Hyo Min and Junghun 2022). Second, fast high-latitude component of the stratosphere-troposphere exchange (Liang et al. 2009) could support the similar observation, as pointed out recently for the AD 993 event (Miyake et al. 2022) and discussed in relation

https://doi.org/10.1017/RDC.2026.10195 Published online by Cambridge University Press

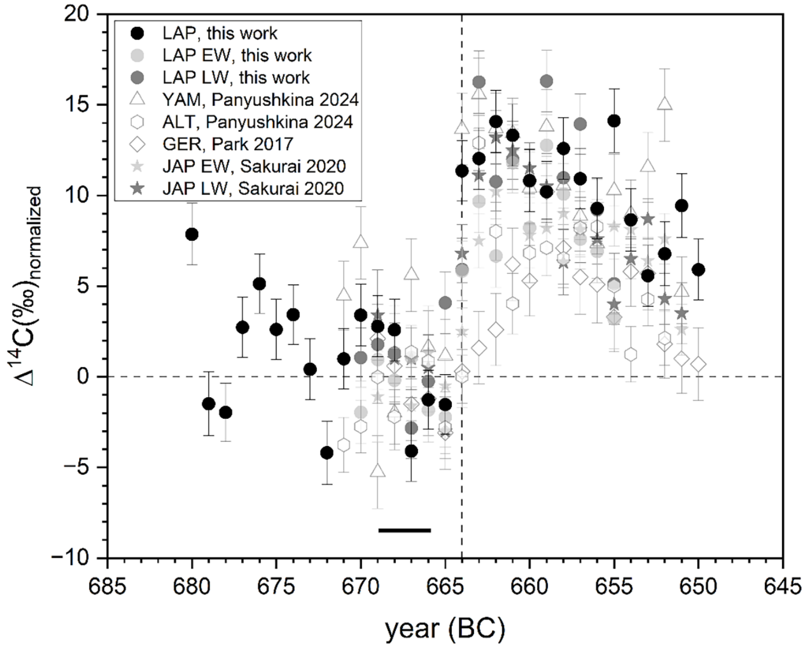

Figure 3. *Annual and subannual results of LAP compared to datasets of Altai (ALT) and Yamal (YAM) (Panyushkina et al. 2024), Germany (GER) (Park et al. 2017) and Japan (JAP) (Sakurai et al. 2020). The data have been normalized by setting the mean of 669–666 BC to equal to 0 to remove potential baseline difference. The dashed horizontal and vertical lines are for guiding the eye corresponding to zero baseline and the year 664 BC, respectively. The horizontal solid line shows the years used for normalization.*

to the transient offset of AD 1860s (Uusitalo et al. 2024). Such early increases have also been observed at high latitudes for the AD 774/775 event in Lapland (Uusitalo et al. 2018) and in Yamal (Jull et al. 2014). Indeed, the rise of the annual ^{14}C signal in 664 BC and in AD 774 is fast in both sites of LAP and YAM (Figure 4).

Taken together, the accumulating observational data suggests that for Miyake events, the increase in ^{14}C begins earlier at high latitudes than at lower latitudes. These observations indicate fast partial transfer of polar ^{14}C into the troposphere at high latitudes by direct tropospheric production or fast transfer across the tropopause, making it available for photosynthetic fixation by trees. In addition, full peak intensities and dilution of the ^{14}C signal at lower latitudes are obtained when the mainly stratospheric air masses eventually reach the lower latitude troposphere with vast atmospheric volume. These components together would contribute to the observed full peak shape.

Previously, prolonged rise time of the ~660 BC event has been attributed to two consecutive SPEs (Panyushkina et al. 2024; Park et al. 2017; Sakurai et al. 2020). Qualitatively, however, the peak shapes of the ~660 BC and AD 774 events (Figure 4; Supplementary Figure S1 for EW-LW comparison) appear similar, with the AD 774 event displaying higher amplitude and magnitude. This challenges the idea of multiple SPEs as a cause of the ~660 BC event's peak shape. Moreover, no such double peaks have been proposed to explain the AD 774 event. Nevertheless, carbon cycle box model analyses were performed to see whether there would be any shape differences due to the assumption of two peaks. We hypothesized that SPEs are the cause of $\Delta^{14}C$ peaks and conducted a detailed analysis of the SPEs producing the peak using an 11-box global carbon cycle model (Güttler et al. 2015).

The simulation results for 1 or 2 SPEs are shown in the graphs of Figure 5 and Table S1. In all scenarios, the timing of the first SPE is assumed to be in February of 665 BC, thus earlier compared to previous analyses (Sakurai et al. 2020). We assume that the duration of all SPEs is one or two days,

https://doi.org/10.1017/RDC.2026.10195 Published online by Cambridge University Press

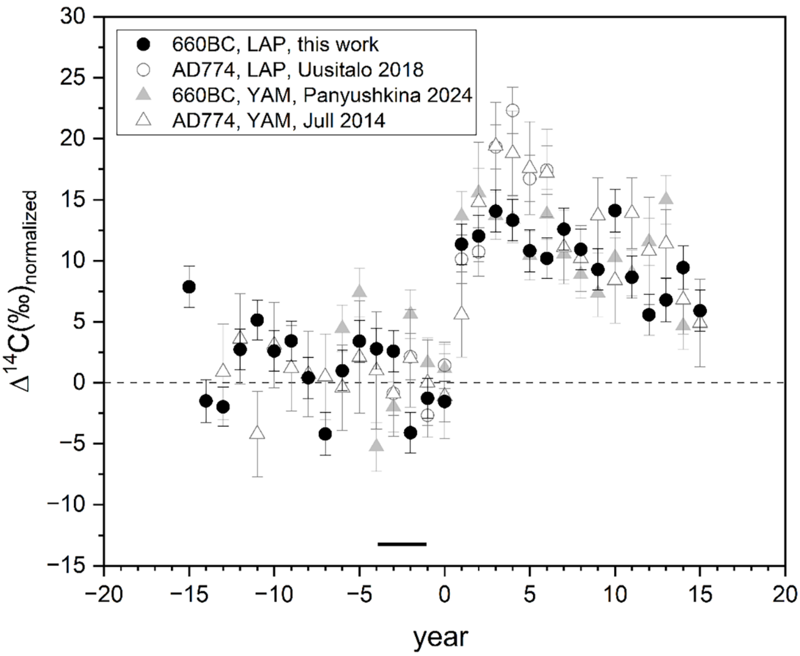

Figure 4. *Comparison between Δ^{14}C data of AD 774 (YAM: Jull et al. 2014, LAP: Uusitalo et al. 2018) and ~660 BC (YAM: Panyushkina et al. 2024, LAP: this work) events at high latitudes. The data has been normalized by setting the mean of 669–666 BC to equal to 0 to remove potential baseline difference. The point of origin is placed at 665 BC and AD 773 for ~660 BC and AD 774 events, respectively. The horizontal solid line shows the years used for normalization.*

although the scan range of the duration of SPEs is allowed to be up to 365 days. An SPE's duration of one or two days is reasonable, as SPE durations are typically a few days in present times (Mewaldt et al. 2005). Particularly, we point out that assuming longer SPE durations may not be consistent with the actual observations. Overall, the model calculations reproduce the observed peak shape extremely well.

The small troposphere ratio (12%) assumed is essential to understand the ^{14}C peak shape of the ~660 BC event and the appearance of a fast Δ^{14}C signal only at high latitudes. Since most (88%) ^{14}C is produced in the stratosphere, the full mixing between stratosphere and troposphere takes longer. In other words, if the energy spectrum of the SPE_{660BC} was softer than that of SPE_{AD774}, the ~660 BC peak may appear slightly delayed in comparison. Interestingly, the same mechanism could also help to explain the transient ^{14}C offset observed between high- and mid-latitude trees around the Carrington event (Uusitalo et al. 2024). For a less energetic event with a soft energy spectrum, ^{14}C production would occur almost exclusively in the high-latitude and -altitude stratosphere. This could significantly prolong the stratosphere-troposphere transport and mixing time, leaving a distinct signal only in the polar regions closest to the production, with its subsequent dilution into larger atmospheric volumes generating the offset observed between records. Unfortunately, a rigorous statistical validation of this hypothesis is not yet possible due to the lack of sufficient data.

χ^2 values of all the three scenarios are almost identical (Table S3). Thus, the used carbon cycle box model is not sufficiently sensitive to clarify the number of SPEs behind the peak shape. This is in accord with our qualitative observation of the peak shape of ~660 BC event: it is actually challenging to observe statistically meaningful differences between the high latitude data of ~660 BC and AD 774 (Figure 4). On one hand, this suggests that more data on individual sites should be collected to obtain better statistical evidence on the peak shapes of Miyake events, similarly as performed for the AD 1860s by Uusitalo et al. (2024). On the other hand, assuming a variable number of production pulses in carbon

https://doi.org/10.1017/RDC.2026.10195 Published online by Cambridge University Press

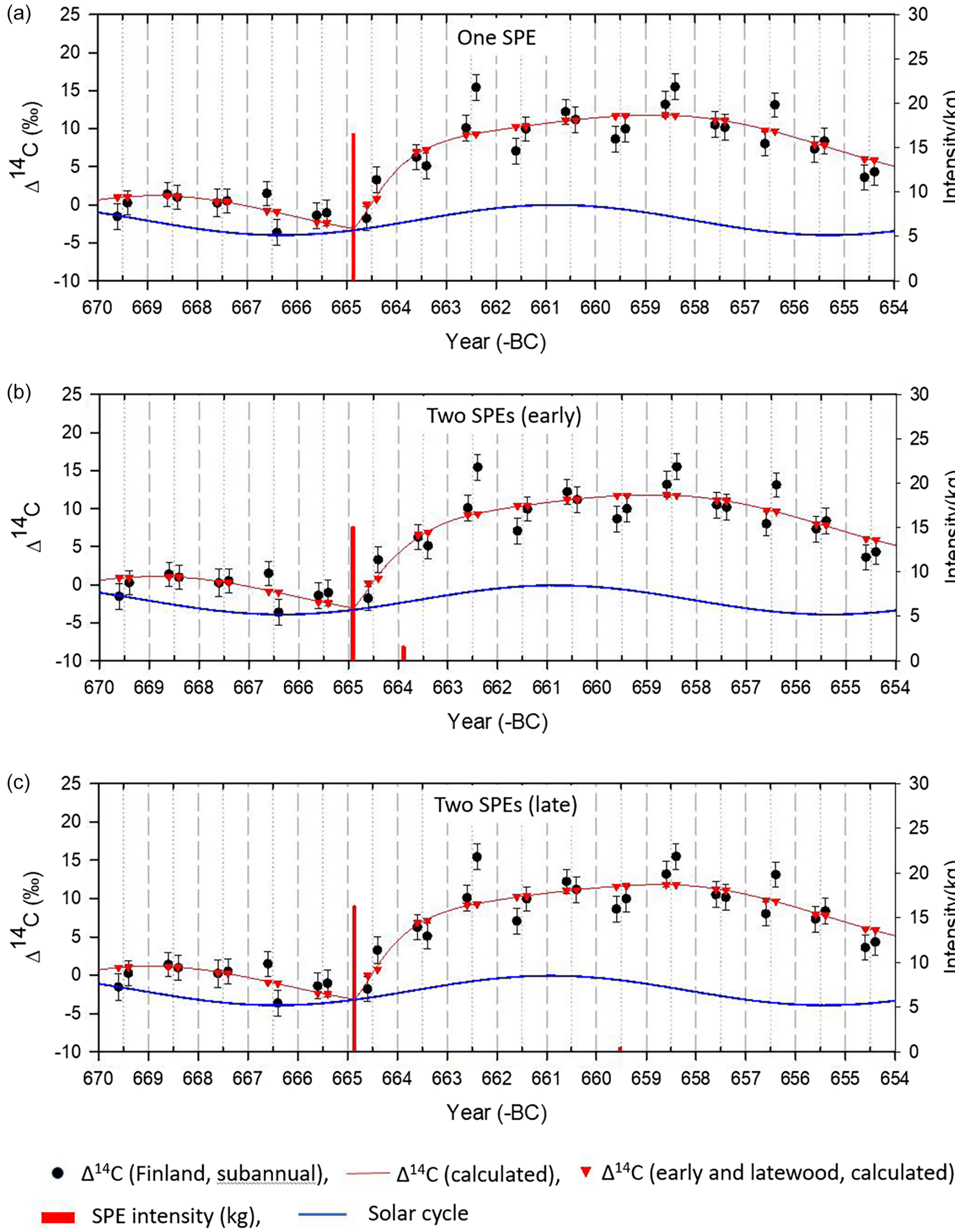

Figure 5. *The simulation result with one and multiple SPEs. Note that the intensity (^{14}C produced in the atmosphere) of SPE in 660 BC of (c) is very small in the model calculation.*

cycle box models may not be a fruitful approach for understanding the peak shapes, particularly at different latitudes. Latitude-dependent rise times and peak magnitudes do not necessarily indicate a number of production pulses, but tell more about the dynamics in the CO_2 transfer from the production areas of ^{14}C into the vast air masses in the troposphere and lower latitudes. Therefore, we urge for development of dynamic carbon cycle models to account for the potentially rapid polar transfer of stratospheric CO_2 into the troposphere to be photosynthetically fixed. Such model could incorporate

https://doi.org/10.1017/RDC.2026.10195 Published online by Cambridge University Press

large-scale and slower stratosphere-troposphere exchange needed to characterize the dilution of ^{14}C signal among larger volumes of air in subpolar troposphere.

Conclusions

The amplitude of the $\Delta^{14}C$ peak at ~660 BC observed in high-latitude trees from Finnish Lapland is about 15‰ and reaches its maximum around 662–661 BC. Subannual data show that $\Delta^{14}C$ starts to increase in the latewood of 665 BC, which is earlier than at lower latitudes. After the baseline adjustment, the annual 664 BC $\Delta^{14}C$ data show a more pronounced increase at high-latitude sites than at lower latitudes, mirroring what was observed for the AD 774 and AD 993 events and suggesting an involvement of a fast component for the polar stratosphere-troposphere exchange. Model simulations indicate that either one or two SPEs could account for the ~660 BC peak, but they do not definitively distinguish between these scenarios. Overall, we note that for high latitudes, the shape of the peak appears very similar to that of the AD 774 event, challenging the need to invoke multiple SPEs or more exotic explanations and instead suggesting the combined influence of the event's initial ^{14}C production characteristics and subsequent atmospheric transport dynamics. Finally, although the commonly used carbon cycle box models are useful for understanding and quantifying the general peak behavior, they appear inadequate to explain regional differences, highlighting the need for more dynamic models.

Supplementary material. To view supplementary material for this article, please visit https://doi.org/10.1017/RDC.2026.10195

Acknowledgments. This research was supported by the Basic Research Project of the Korea Institute of Geoscience and Mineral Resources (KIGAM), funded by the Ministry of Science and ICT (GP2020-019). The work of Laboratory of Chronology and Natural Resources Institute Finland has been supported by the Research Council of Finland projects QUANOMAL and WELT (288083, 288267, 355266, 355268). LLM-based AI tools were used for writing assistance and grammar checking when preparing this manuscript.

Competing interests. The authors declare no conflicts of interest.

References

Bard E, Miramont C, Capano M et al. (2023) A radiocarbon spike at 14,300 cal yr BP in subfossil trees provides the impulse response function of the global carbon cycle during the Late Glacial. *Philosophical Transactions of the Royal Society A* **381**, 20220206.

Brehm N, Bayliss A, Christl M, Synal H-A, Adolphi F, Beer J, Kromer B, Muscheler R, Solanki SK, Usoskin I, Bleicher N, Bollhalder N, Bollhalder S, Tyers C and Wacker L (2021) Eleven-year solar cycles over the last millennium revealed by radiocarbon in tree rings. *Nature Geoscience* **14**, 10–15.

Brehm N, Christl M, Knowles TDJ et al. (2022) Tree-rings reveal two strong solar proton events in 7176 and 5259 BCE. *Nature Communications* **13**, 1196. doi: 10.1038/s41467-022-28804-9.

Büntgen U, Lukas W, Galván JD et al. (2018) Tree rings reveal globally coherent signature of cosmogenic radiocarbon events in 774 and 993 CE. *Nature Communications* **9**, 3605. doi: 10.1038/s41467-018-06036-0.

Golubenko K, Rozanov E, Kovaltsov G and Usoskin I (2022) Zonal mean distribution of cosmogenic isotope (^{7}Be, ^{10}Be, ^{14}C, and ^{36}Cl) production in stratosphere and troposphere. *Journal of Geophysical Research: Atmospheres* **127**, e2022JD036726. doi: 10.1029/2022JD036726.

Güttler D, Adolphi F, Beer J et al. (2015) Rapid increase in cosmogenic ^{14}C in AD 775 measured in New Zealand kauri trees indicates short-lived increase in ^{14}C production spanning both hemispheres. *Earth and Planetary Science Letters* **411**, 290–297.

Hambaryan VV and Neuhäuser R (2013) Galactic short gamma-ray burst as cause for the ^{14}C peak in AD 774/5. *Monthly Notices of the Royal Astronomical Society* **430**, 32–36.

Hong W, Park JH, Sung KS, Woo HJ, Kim JK, Choi HW and Kim GD (2010a) A new 1MV AMS facility at KIGAM. *Radiocarbon* **52**(2), 243–251. doi: 10.1017/S0033822200045276.

Hong W, Park JH, Kim KJ, Woo HJ, Kim JK, Choi HW and Kim GD (2010b) Establishment of chemical preparation methods and development of an automated reduction system for AMS sample preparation at KIGAM. *Radiocarbon* **52**(3), 1277–1287. doi: 10.1017/S0033822200046361.

Hua Q, Barbetti M and Rakowski AZ (2013) Atmospheric radiocarbon for the period 1950–2010. *Radiocarbon* **55**(4), 2059–2072.

Hyo Min L and Junghun P (2022) Solar and galactic ^{14}C production rates in atmosphere using an MCNP6 simulation. *Journal of Radioanalytical and Nuclear Chemistry* **331**, 5667–5674.

https://doi.org/10.1017/RDC.2026.10195 Published online by Cambridge University Press

Jull AJT, Panyushkina IP, Lange TE, Kukarskih VV, Myglan VS, Clark KJ, Salzer MW, Burr GS and Leavitt SW (2014) Excursions in the ^{14}C record at AD 774–775 in tree rings from Russia and America. *Geophysical Research Letters* **41**. doi: 10.1002/2014GL059874.

Jull AJT, Panyushkina I, Miyake F, Masuda K, Nakamura T, Mitsutani T, Lange TE, Cruz RJ, Baisan C, Janovics R, Varga T and Molnár M (2018) More rapid ^{14}C excursions in the tree-ring record: A record of different kind of solar activity at about 800 BC? *Radiocarbon* **60**(4), 1237–1248. doi: 10.1017/RDC.2018.53.

Levin I, Kromer B, Schoch-Fischer H, Bruns M, Münnich M, Berdau D, Vogel JC and Münnich KO (1985) 25 years of tropospheric ^{14}C observations in central Europe. *Radiocarbon* **27**(1), 1–19.

Liang Q, Douglass AR, Duncan BN, Stolarski RS and Witte JC (2009) The governing processes and timescales of stratosphere-to-troposphere transport and its contribution to ozone in the arctic troposphere. *Atmospheric Chemistry and Physics* **9**(9), 3011–3025. doi: 10.5194/acp-9-3011-2009.

Mekhaldi F, Muscheler R, Adolphi F et al. (2015) Multiradionuclide evidence for the solar origin of the cosmic-ray events of AD 774/5 and 993/4. *Nature Communications* **6**, 8611. doi: 10.1038/ncomms9611.

Melott AL and Thomas BC (2012) Causes of an AD 774–775 ^{14}C increase. *Nature* **491**, E1–E2.

Mewaldt RA, Cohen CMS, Labrador AW, Leske RA, Mason GM, Desai MI, Looper MD, Mazur JE, Selesnick RS and Haggerty DK (2005) Proton, helium, and electron spectra during the large solar particle events of October-November 2003. *Journal of Geophysical Research* **110**, A09S18. doi: 10.1029/2005JA011038.

Miyahara H, Tokanai F, Moriya T et al. (2022) Recurrent large-scale solar proton events before the onset of the Wolf grand solar minimum. *Geophysical Research Letters* **49**, e2021GL097201.

Miyake F, Nagaya K, Masuda K and Nakamura T (2012) A signature of cosmic-ray increase in AD 774–775 from tree rings in Japan. *Nature* **486**, 240–242.

Miyake F, Masuda K and Nakamura T (2013) Another rapid event in the carbon-14 content of tree rings. *Nature Communications* **4**, 1748. doi: 10.1038/ncomms2783.

Miyake F, Jull AJT, Panyushkina IP, Wacker L, Salzer M, Baisan CH, Lange T, Cruz R, Masuda K and Nakamura T (2017) Large ^{14}C excursion in 5480 BC indicates an abnormal sun in the mid-Holocene. *Proceedings of the National Academy of Sciences of the United States of America* **114**(5), 881–884.

Miyake F, Panyushkina IP, Jull AJT, Adolphi F, Brehm N, Helama S, Kanzawa K, Moriya T, Muscheler R, Nicolussi K, Oinonen M, Salzer M, Takeyama M, Tokanai F and Wacker (2021) A single-year cosmic ray event at 5410 BCE registered in ^{14}C of tree rings. *Geophysical Research Letters* **48**, e2021GL093419.

Miyake F, Hakozaki M, Kimura K, Tokanai F, Nakamura T, Takeyama M and Moriya T (2022) Regional differences in carbon-14 data of the 993 CE cosmic ray event. *Frontiers in Astronomy and Space Sciences* **9**, 886140. doi: 10.3389/fspas.2022.886140.

Nydal R (1968) Further investigation on the transfer of radiocarbon in nature. *Journal of Geophysical Research* **73**(12), 3617–3635.

O'Hare P et al. (2019) Multiradionuclide evidence for an extreme solar proton event around 2,610 B.P. (~660 BC). *Proceedings of the National Academy of Sciences* **116**(13), 5961–5966.

Paleari C, Mekhaldi F, Adolphi F et al. (2022) Cosmogenic radionuclides reveal an extreme solar particle storm near a solar minimum 9125 years BP. *Nature Communications* **13**, 214. doi: 10.1038/s41467-021-27891-4.

Panyushkina IP, Jull AJT, Molnár M, Varga T, Kontul I, Hantemirov R, Kukarskih V, Sljusarenko I, Myglan V and Livina V (2024) The timing of the ca-660 BCE Miyake solar-proton event constrained to between 664 and 663 BCE. *Communications Earth & Environment* **5**, 454. doi: 10.1038/s43247-024-01618-x.

Park J, Seo J-W, Hong W, Park G, Sung K, Park YJ and Kim Y-J (2020) Estimation of the occurrence time of the Δ^{14}C peak in AD 775 based on the oxidation time of ^{14}C in the atmosphere and Δ^{14}C values in subannual tree rings. *Radiocarbon* **62**(5), 1285–1298. doi: 10.1017/RDC.2020.69.

Park J, Southon J, Fahrni S, Creasman PP and Mewaldt R (2017) Relationship between solar activity and Δ^{14}C peaks in AD 775, AD 994, and 660 BC. *Radiocarbon* **59**(4), 1147–1156. doi: 10.1017/RDC.2017.59.

Pavlov AK, Blinov AV, Frolov DA, Konstantinov AN, Koudriavtsev IV, Ogurtsov MG, Ostryakov VM and Vasilyev (2019) Isotopic imprint of the Solar system encounter with interstellar gas cloud around 660 BC (2610 BP). *Journal of Physics: Conference Series* **1400**, 022034.

Pavlov AK, Blinov AV, Konstantinov AN, Ostryakov VM, Vasilyev GI, Vdovina MA and Volkov PA (2013) AD 775 pulse of cosmogenic radionuclides production as imprint of a Galactic gamma-ray burst. *Monthly Notices of the Royal Astronomical Society* **435**, 2878–2884.

Rakowski AZ, Pawlyta J, Miyahara H, Krąpiec M, Molnár M, Wiktorowski D and Minami M (2024) Radiocarbon concentration in sub-annual tree rings from Poland around 660 BCE. *Radiocarbon* **66**(6), 1981–1990. doi: 10.1017/RDC.2023.79.

Sakurai H, Tokanai F, Miyake F, Horiuchi K, Masuda K, Miyahara H, Ohyama M, Sakamoto M, Mitsutani T and Moriya T (2020) Prolonged production of ^{14}C during the ~660BC solar proton event from Japanese tree rings. *Scientific Reports* **10**, 660.

Terrasi F, Marzaioli F, Buompane R, Passariello I, Porzio G, Capano M, Helama S, Oinonen M, Nöjd P, Uusitalo J, Jull AJT, Panyushkina IP, Baisan C, Molnar M, Varga T, Kovaltsov G, Poluianov S and Usoskin I (2020) Can the ^{14}C production in 1055 CE be affected by SN 1054? *Radiocarbon* **62**(5), 1403–1418.

Usoskin IG, Kromer B, Ludlow F, Beer J, Friedrich M, Kovaltsov GA, Solanki SK and Wacker L (2013) The AD775 cosmic event revisited: The Sun is to blame. *Astronomy & Astrophysics* **552**, L3. doi: 10.1051/0004-6361/201321080.

Uusitalo J, Arppe L, Hackman T, Helama S, Kovaltsov G, Mielikäinen K, Mäkinen H, Nöjd P, Palonen V, Usoskin I and Oinonen M (2018) Solar superstorm of AD 774 recorded subannually by Arctic tree rings. *Nature Communications* **9**(1), 3495.

https://doi.org/10.1017/RDC.2026.10195 Published online by Cambridge University Press

Uusitalo J, Arppe L, Helama S, Mizohata K, Mielikäinen K, Mäkinen H, Nöjd P, Timonen M, and Oinonen M (2022) From lakes to ratios: ^{14}C measurement process of the Finnish tree-ring research consortium. *Nuclear Instruments and Methods in Physics Research B* **519**, 37–45.

Uusitalo J, Golubenko K, Arppe L, Brehm N, Hackman T, Hayakawa H, Helama S, Mizohata K, Miyake F, Mäkinen H, Nöjd P, Tanskanen E, Tokanai F, Rozanov E, Wacker L, Usoskin I and Oinonen M (2024) Transient offset in ^{14}C after the Carrington Event recorded by polar tree rings. *Geophysical Research Letters* **51**, e2023GL106632. doi: 10.1029/2023GL106632.

Yasuike K, Yamada Y and Komura K (2008) Long-term variation of ^{14}C concentration in atmospheric CO_2 in Japan from 1991 to 2000. *Journal of Radioanalytical and Nuclear Chemistry* **275**, 313–323.

Cite this article: Park J, Uusitalo J, Hong W, Park G, Sung K, Hackman T, Helama S, Mäkinen H, Nöjd P, and Oinonen M (2026). (2026). Early ^{14}C increase in high-latitude trees at 665–664 BC. *Radiocarbon* **68**, 382–391. https://doi.org/10.1017/RDC.2026.10195

https://doi.org/10.1017/RDC.2026.10195 Published online by Cambridge University Press